Article:
Alresheedi, MT, Hussein, AT orcid.org/0000-0002-2519-082X and Elmirghani, JMH (2017) Uplink Design in VLC Systems with IR Sources and Beam Steering. IET Communications, 11 (3). pp. 311-317. ISSN 1751-8628

https://doi.org/10.1049/iet-com.2016.0495

Uplink Design in VLC Systems with IR Sources and Beam Steering

Mohammed T. Alresheedi[1], Ahmed Taha Hussein[2] and Jaafar M. H. Elmirghani[2] Fellow of IET
[1] Department of Electrical Engineering, King Saud University, Riyadh, Kingdom of Saudi Arabia
[2]School of Electronic and Electrical Engineering, University of Leeds, Leeds LS2 9JT, UK
[*] malresheedi@ksu.edu.sa

Abstract: The need for high-speed local area networks to meet the recent developments in multimedia and video transmission applications has recently focused interest on visible light communication (VLC) systems. Although VLC systems provide lighting and communications simultaneously from light emitting diodes, LEDs, the uplink channel design in such a system is a challenging task. In this paper, we propose a solution in which the uplink challenge in indoor VLC is resolved by the use of an Infrared (IR) link. We introduce a novel fast adaptive beam steering IR system (FABS-IR) to improve the uplink performance at high data rates while providing security for applications. The goal of our proposed system is to enhance the received optical power signal, speed up the adaptation process and mitigate the channel delay spread when the system operates at a high transmission rate. The channel delay spread is minimised from 0.22 ns given by hybrid diffuse IR link to almost 0.07 ns. At 2.5 Gb/s, our results show that the imaging FABS-IR system accomplished about 11.7 dB signal to noise ratio (SNR) in the presence of multipath dispersion, receiver noise and transmitter mobility.

Index Terms— uplink channel, beam steering IR, delay spread, SNR.

1. Introduction

The large and continuous growth in mobile devices including smart phones, laptops, and Internet of Things (IoT) devices is driving a huge demand for data access to wireless networks. Visible light communication (VLC) is becoming more popular everyday due to its inherent advantages over radio frequency (RF) systems. The advantages include a large unregulated spectrum, simple receivers (silicon photo detectors), simple transmitters (light emitting diodes, LEDs), freedom from fading, confidentiality and immunity against interference from electrical devices. The concept of VLC systems revolves around

the use of light emitting diodes (LEDs) for both lighting and communications. The main drives for this new technology include the recent development of solid state lighting, longer lifetime of high brightness LEDs compared to other artificial light sources such as florescent and incandescent light bulbs, high data rate, low power consumption and green communications [1]-[5].

Apart from the advantages of a large potential bandwidth, VLC makes it possible to reuse the same wavelength in other parts of an indoor environment without facing any interference and security problems and this is due to the fact that VLC signals cannot penetrate walls or other opaque barriers [6]. However, the VLC system is not without drawbacks; there are two major limitations in VLC systems. The first is the low modulation bandwidth of the LEDs, which limits the transmission data rates. The second is the spread of the received pulse due to the reflections from walls and ceiling in an indoor environment which causes multipath dispersion that leads to inter symbol interference (ISI). Different techniques have been suggested to overcome the limitations in VLC systems (ISI and low modulation bandwidth of LEDs ISI), so that higher data rates can be realised. Previous work in [7] proposed a 3 Gb/s VLC link that uses a Gallium Nitride μLED and orthogonal frequency division multiplexing (OFDM). OFDM is employed as a modulation scheme and pre- and post-equalisation techniques, as well as adaptive data loading are applied in order to achieve 3 Gb/s. Elmirghani and his group have recently improved performance of VLC systems by replacing LEDs with Laser diodes (LDs) and integrated the system with the imaging diversity receiver [8]-[11]. A 10 Gb/s indoor VLC in a realistic environment has been shown to be possible by using a delay adaptation approach, LDs and imaging receiver [8]. The system in [8] used a simple modulation format (On Off Keying (OOK)) and avoid any complex wavelength division multiplexing (WDM) techniques. Moreover, a VLC relay assisted system is used with a delay adaptation technique and an imaging receiver to further improve the VLC system performance [11]. These efforts aim to achieve the highest data rates possible.

Most of the current and previous work on VLC focuses mainly on the downlink channel. The primary goal of VLC downlink design is to enhance data rates within the constraints of VLC as discussed above. Although VLC systems provide lighting and communications simultaneously from LEDs, the uplink channel design in such a system is challenging task. This is due to the energy limitations of mobile devices (where such light does not need to be generated for illumination) and also due to the potential glare from the light where VLC signals can cause discomfort to human eyes and affect the indoor illumination. Taking these reasons into considerations, VLC systems remain a strong candidate for downlink implementation within a local network. However, it is better if VLC technology is complemented with an alternative uplink technology.

Recent work in [12] proposed a hybrid solution where the uplink challenge is resolved by the use of RF-VLC combination. The system comprised of WiFi uplink and VLC downlink in order to increase the overall capacity with multiple users. This solution is suitable for RF insensitive areas such as schools and homes with relatively small data rates. Moreover, different researchers have demonstrated a bi-directional indoor communication system based on VLC red-green-blue RGB-LEDs [13]. Each colour can be used to carry different signals. The study has achieved 300 Mb/s uplink transmission rate. However, this type of configuration requires a directional transmission beam that can lead to significant deterioration of throughput given the potential movement of users. Also the uplink VLC can produce light which is uncomfortable to human eyes. Therefore, there is a need to find alternative solutions with relatively high transmission speed in sensitive places and high-security applications. In this paper, we propose Infrared (IR) uplink channel design to overcome the potential issues of uplink transmission in VLC systems. IR (Infrared) optical communications has the same advantages as VLC systems. It has also some additional advantages compared to VLC. For example light dimming is not an issue in IR systems and the uplink implementation using IR is convenient as it avoids bright visible light next to the user equipment, next to a laptop for example. It can also provide high transmission rates similar to VLC systems and potentially

higher data rates (data rate up to 10 Gb/s employing OOK modulation can be achieved) [14], [15]. This is mainly because of the modulation bandwidth of LD used in IR systems which is wider than the white LEDs.

In this paper, we propose a hybrid conventional diffuse IR (HCD-IR) uplink system in which the optical signals can be fully diffuse over the entire environment. Diffuse systems offer great link stability as well as providing substantial immunity to direct beam blockage near to the receiver. Furthermore, a diffuse connection permits users to immediately join and collaborate with the use of mobile computers, wireless printers, modems, and office and home networking devices. However, diffuse systems may suffer from multipath dispersion, and this may cause signal spread and ISI. A direct IR link with a narrow beam can be used to overcome this issue. However, a perfect alignment between the transmitter and the receiver is required in order to establish such a link, and can be easily disconnected due to the user's motion. In order overcome this issue, we propose a novel fast adaptive beam steering IR system (FABS-IR) to improve the uplink performance at high data rates. To minimise the complexity of the design, we propose an adaptive finite vocabulary stored hologram for beam steering by using of simulated annealing optimisation. In this work, we propose the use of holograms and beam steering in uplink IR-VLC systems with efficient adaptation. The idea of finite adaptive stored holograms has been introduced first in downlink multi-spot diffusing IR systems (non-direct line-of-sight) in [16] and it is applied here for the first time to uplink visible light communication (VLC) systems. To the extent of our knowledge, 1.25 Gb/s and 2.5 Gb/s data rates, the highest data rates to date for an uplink VLC system are accomplished by using our new systems (with simple modulation format OOK).

The paper is organised as follows: Section 2 explains system configurations. The system model and simulation set-up are given in Section 3. The simulation results of our proposed system are given and discussed in Section 4. Finally, conclusions are drawn in Section 5.

2. System Configurations

In this section, we focus on the design of the uplink in VLC and consider the use of an IR link. The downlink design, for VLC systems, has been evaluated in our work in [8]-[11]. Fig. 1 shows IR optical wireless communication architecture for the uplink VLC system. The transmitter is placed on the communication plane (CP) while the receiver (controller) faces downward at the centre of ceiling. The controller is linked with all LEDs via fibre links (to link to the main network in the building). Two uplink transmitter configurations: HCD-IR and FABS-IR in conjunction, with non-imaging and imaging receiver, are studied, evaluated and compared in order to find the best uplink design for indoor VLC systems.

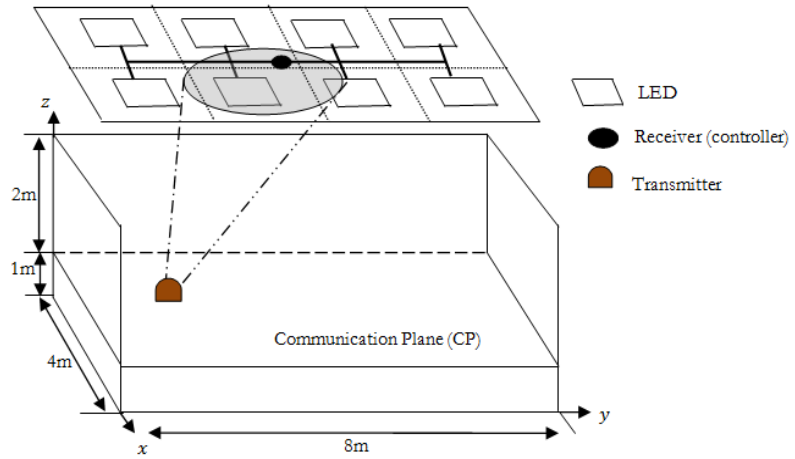

Fig. 1: Architecture of our proposed IR uplink system.

A. HCD-IR Transmitter

The basic hybrid conventional diffuse IR transmitter (HCD-IR) employs diffuse transmission and a wide field of view (FOV) receiver. It uses direct and non-direct paths between the receiver and the transmitter. The HCD-IR does not rely on a direct line of sight (LOS), which permits the uplink VLC system to operate even when the receiver is obstructed from the transmitter. However, a pure diffuse system coupled with a wide FOV receiver is subject to multipath dispersion, which may result in pulse spreading and extreme ISI. The diffuse HCD-IR system employs a large beam transmitter with a large reception angle (FOV=90°) at the receiver end.

B. FABS-IR Transmitter

Angle adaptation technique, based on liquid crystal devices, has been introduced for the first time in a downlink IR communication system to improve the SNR at the receiver [14], [15]. It is considered to be a powerful approach that can help the transmitter to optimise the distribution of spots and to find the best location of the spots regardless of the receiver's location, the transmitter's position and the receiver's reception angle. However, this technique requires more time for calculations on a typical digital signal processor to generate a hologram at each step. In our new fast adaptive (FABS-IR) system, we propose an adaptive IR stored hologram technique in order to steer the beams in uplink IR-VLC systems. In a typical office space with dimension of $8\text{ m} \times 4\text{m}$ ($y\text{ m} \times x\text{ m}$), the floor (or ceiling) is divided into small areas, i.e. 512 regions where each area has dimension of $0.25\text{ m} \times 0.25\text{ m}$. The total number of holograms to be stored in uplink design is N, where N is the number of areas into which the ceiling or floor is divided. This large number of regions has been selected in order to help the transmitter to find the exact receiver position during mobility. In our case, the receiver is fixed (i.e., stationary) at the centre of the room while the transmitter is mobile and uses a stored hologram that steers the beam (narrow direct LOS link) to the optimum location if the transmitter is present in any one of the regions. The idea of finite stored holograms has been recently introduced in IR diffusing spot systems and VLC systems [16]-[18] and it is developed here for the first time in the uplink VLC in order improve the performance of the IR-VLC system as well as speed up the adaptation process. The hologram phase and pattern distribution were calculated in a similar fashion to those used in [16]. More details about the characteristic and the design of hologram can be found in our recent works in [18]. Three snapshots of the hologram reconstruction intensity and phase distributions in the far field at different iterations are shown in Fig. 2. The reconstruction intensities are improved when the number of iterations increases. This is attributed to the use of simulated annealing which attempts to reduce the cost function, hence improving hologram phases leading to more accurate spot location/beam steering. Fig. 3 shows the cost function versus the number of iterations completed.

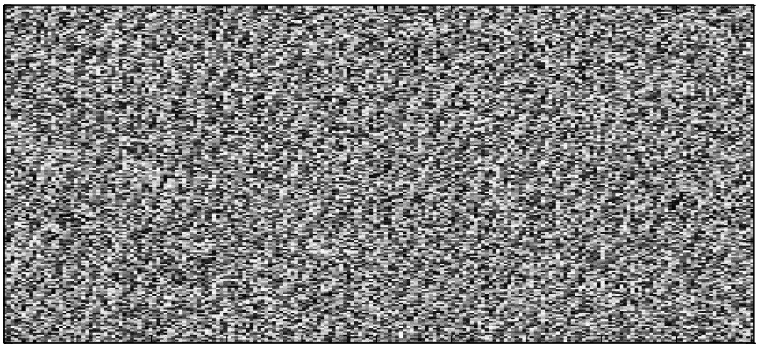

Phase of hologram at iteration 5

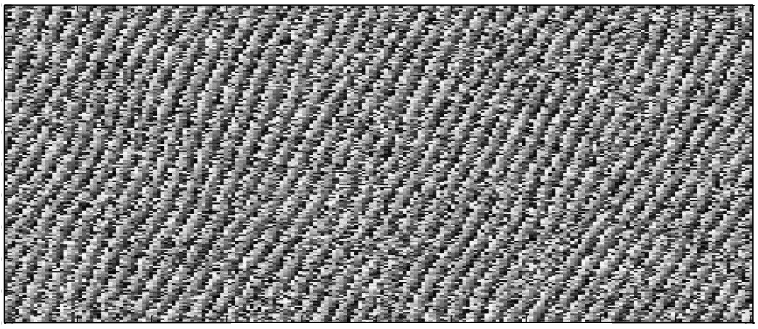

Phase of hologram at iteration 15

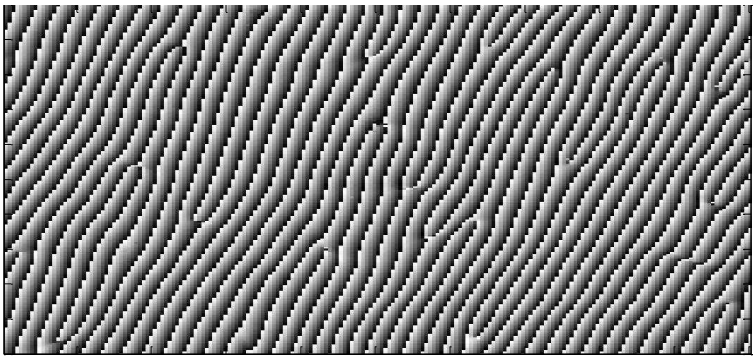

Phase of hologram at iteration 100

Fig. 2: The phase pattern of hologram at iterations: 5, 15 and 100, phase levels represented by different gray levels in the range of 0 (black) to 2π (white).

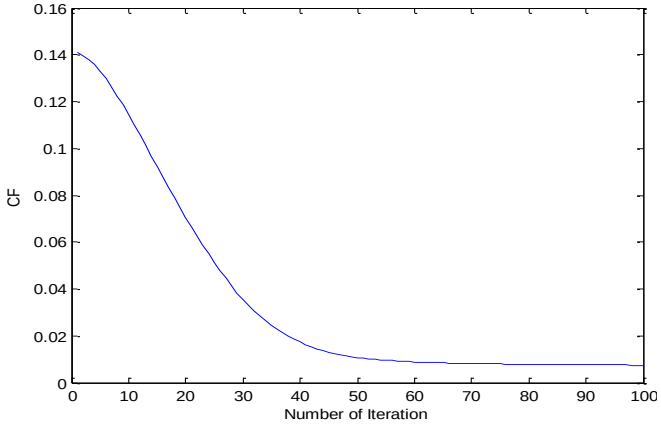

Fig. 3: Number of iterations versus cost function.

In the case of classic beam steering the adaptive transmitter first scans all N holograms (where the total number of holograms used in this case is N=512). The receiver records the SNR associated with each hologram; this information is then sent back to the transmitter in order to assist the transmitter in selecting the best hologram. Usually the adaptive transmitter selects holograms based on their associated SNRs with the hologram providing the best SNR being selected. However, scanning all the stored holograms in the system negatively causes an exhaustive search mechanism. The high quantity of stored holograms in the proposed system leads to increase in the time needed for the adaptation process. If each hologram requires 1 ms in order to calculate its SNR (based on a typical processor) then the total time needed (adaptation time) to find the best hologram when the receiver moves is 512 ms. Introducing a fast adaptive search algorithm (based on a divide and conquer (D&C) algorithm) resolves this issue, and improves the SNR. This is accomplished through the use of more holograms while simultaneously decreasing the required computation time needed to select the optimum hologram. The D&C algorithm has been first introduced and explained in a downlink VLC system in [16]-[18] and it is adapted here for the first time in uplink channel. Our fast adaptive algorithm is based on a D&C algorithm to find the optimum hologram that achieves the highest receiver SNR. The following presents our adaptive proposed FABS-IR algorithm utilised in a single user scenario:

1- Firstly, based on the hologram transmission angles, the adaptive transmitter splits the stored holograms into four quadrants. The transmission angles correlated with the first quadrant are $\delta_{\max-x}$ to 0 in the x-axis and $\delta_{\max-y}$ to 0 in y-axis.

2- In order to identify the first sub-optimum hologram, the adaptive transmitter scans the middle holograms in each quadrant.

3- The receiver estimates the SNR and then sends (feedback signal) information of the SNR associated with each hologram back to the transmitter. It should be noted that in order to identify the first sub-optimal region, four holograms will first be scanned.

4- The adaptive transmitter stores the hologram transmission angles where the receiver SNR is sub-optimal. In the case that the transmitter receives more than one equally optimal SNR due to the room symmetry, or due to both the transmitter and receiver being co-allocated (receiver on the boundary of the optimum region), then the transmitter selects the first hologram from among the available equally good hologram choices and discard the others.

5- The quadrant which includes the sub-optimal hologram is selected for the next cycle by the adaptive transmitter.

6- The adaptive transmitter sub-divides the sub-optimal quadrant into four sub-quadrants, in order to find the second sub-optimal quadrant, steps 3 to 5 are repeated.

7- The second sub-optimal quadrant is again subdivided into four sub-quadrants by the adaptive transmitter. To identify the third sub-optimal quadrant, the transmitter repeats steps 3 to 5.

8- The optimal transmission angles of the hologram that achieved the highest receiver SNR, are determined by the D&C algorithm and the adaptive transmitter.

Table I shows the fast adaptation algorithm, more details and explanations about each step can be found in [19]. The fast proposed system, FABS-IR (with 512 holograms), decreases the computation time taken by the classic angle adaptive holograms, from 512 ms to 28 ms. It reduced the computation time by a factor of 16 in the case of our proposed system. The design complexity associated with our proposed system is discussed in Section 4. It should be noted that a number of different iteration counts of the search algorithm (i.e., three up to six) were tested. However, we found that in most receiver locations the

proposed algorithm is able to determine the optimum location of the receiver by the third iteration. Therefore, we restricted the search algorithm to three iterations to reduce the complexity associated with the computation time required to identify the optimum location. It should be noted that our proposed system operates in an empty rectangular room. In this work, we do not study the potential interference due to sunlight through windows and we do not consider the impact of shadowing in a realistic indoor environment. In the case of a realistic indoor environment, the number of holograms to be scanned in each area should be increased. This will lead to increase in the adaptation process. The interference of daylight through windows is of interest and will be considered in future work.

TABLE I
FABS-IR Algorithm

Inputs: θ_x^{start}=-70° and θ_x^{end}=70° (the lower and higher holograms scan ranges along x-axis).
θ_y^{start}=-70° and θ_y^{end}=70° (the lower and higher holograms scan ranges along y-axis).
θ_{steps}=26.56° (initial value, step size 100 cm)

for i = 0:26.56:140;
  for l = 0:26.56:140;
    $\theta_x = i$; $\theta_y = l$; (Transmission angles in x and y axes)
    Produce a hologram with a direction associated with θ_x and θ_y.
    for S =1: j;
      Calculate and sum the received powers.
      Produce the impulse response $h_j(t)$
      Calculate the pulse response $h_j(t) \otimes P(t - Tb)$ and then calculate $(PS_1 - PS_0)$
      Compute $SNR_j = (\frac{R(P_{S1} - P_{S0})}{\sigma_t})^2$;
    end for
    $SNR\ (i,l) = max\ (SNR_j)$;
    $detector\ (i,l) = find\ (SNR_j) == (max\ (SNR_j))$;
  end for
end for
$SNR_{max} = max\ SNR\ (i,l)$;
$[\theta_{x-sub-optimum}, \theta_{y-sub-optimum}] = find\ (SNR\ (i,l)) == (SNR_{max})$; (identify sub-optimum hologram).
If $|\theta_{x-sub-optimum}| \leq (|\theta_x^{end}| - |\theta_x^{start}|)/2$ (reset new scan range in the x-axis)
$\theta_x^{end} = \theta_{x-sub-optimum}$;
Else
$\theta_x^{start} = \theta_{x-sub-optimum}$;
end If
If $|\theta_{y-sub-optimum}| \leq (|\theta_y^{end}| - |\theta_y^{start}|)/2$ (reset new scan range in the y-axis)
$\theta_y^{end} = \theta_{y-sub-optimum}$;
Else
$\theta_y^{start} = \theta_{y-sub-optimum}$;
end If
$\theta_x^{optimum} = \theta_{x-\text{sub}-\text{optimum}}$; $\theta_y^{optimum} = \theta_{y-\text{sub}-\text{optimum}}$; (identify optimum hologram).

3. Simulation Set-up and System Model

In indoor IR communication links, intensity modulation and direct detection (IM/DD) is a suitable simple approach that is widely used. The indoor IR IM/DD channel can be fully identified and specified by its impulse response $h(t)$ as [14]:

$$I(t) = Rx(t) \otimes h(t) + n_b(t), \quad (1)$$

where $x(t)$ is the emitted optical power and $\otimes$ denotes convolution, R represents the photodetector responsivity and n_b represents the received background noise. The background noise is modelled as white, Gaussian and independent of the received signal. I(t) is the instantaneous current of the photodetector.

The proposed systems, HCD-IR and FABS-IR, were purposely combined with imaging receivers. Simulations were performed for an empty room with dimensions of 4m × 8m × 3m (x m × y m × z m), as shown in Fig. 1. In our work, we assumed that the walls are covered with plaster which is known to reflect light rays in a form close to a Lamertian function [20]. Consequently, walls and ceiling are modelled as Lambertian reflectors that reflect back 80% of the incident energy while the floor is assumed to only reflect 10% of the incident power. In addition, reflections of other structures such as doors and windows are considered to be identical to reflections from walls. The transmitted signal travels to the receiver through multiple reflections from the room's reflecting surfaces. These reflecting surfaces are subdivided into a number of equal-size square-shaped reflecting elements. The reflection elements can be treated as small secondary transmitters that diffuse the incident rays back into the space from their centre. It has been experimentally proven that third-order reflections and above do not contribute significantly to the received optical power [2], [20]-[21]. Based on this information, the simulations include only the first two reflections (i.e., first and second reflections). In this work, the surface elements of 5 cm × 5 cm were used for the first reflections and 20 cm × 20 cm for the second-order reflections. More simulation parameters are given in Table II.

For the hybrid IR system (HCD-IR), the transmitter is pointed upward and transmitted 1 W with an ideal diffuse pattern. Exposure to optical radiation at such power levels can be hazardous to the skin and eyes. Nevertheless, different techniques can be used to reduce the impact of the high laser power such as extending the source size, destroying its spatial coherence using holograms mounted on the transmitter or the use of arrays of transmitters. Pohl. et al. have shown that such a source may use an integrating sphere

TABLE II
SIMULATION PARAMETERS

Parameter	Configuration
	UPLINKS TRANSMISSION
Length	8 m
Width	4 m
Height	3 m
ρ x-z wall	0.8
ρ y-z wall	0.8
ρ x-z op wall	0.8
ρ y-z op wall	0.8
ρ Floor	0.3
	Transmitter
Quantity	1
Elevation	90°
Azimuth	0°
	Imaging Receiver
Quantity	1
Location (x, y, z)	(2m, 4m, 3m)
Detector array's area	2 cm^2
Number of Pixels	200
Area of pixels	1 mm^2
Elevation	90°
Azimuth	0°
Acceptance semi-angle	65°
	Resolutions
Time bin duration	0.5 ns , 0.01ns
Bounces	1 2
Number of elements	32000 2000
Number-of-spot lamps	8
Locations (x,y,z)	(1m,1m,1m), (1m,3m,1m), (1m,5m,1m), (1m,7m,1m)(3m,1m,1m), (3m,3m,1m), (3m,5m,1m), (3m,7m,1m)
Wavelength	850 nm
Preamplifier design	PIN-FET
Bandwidth (BW)	1.25 GHz 2.5 GHz
Bit rate	1.25 Gb/s 2.5 Gb/s

as a diffuser to emit optical powers in the range 100mW – 1W [23]. In the case of fast adaptive stored hologram (FABS-IR) system, the transmitter emitted 150 mW, where the hologram used n= 45 in order to

focus beams within 0.25 m × 0.25 m area. A small transmitted power (150 mW) is used in our fast adaptive hologram system to mitigate the impact of eye safety in the indoor VLC environment [24], [25].

In order to combat the issues of ambient background noise and multipath dispersion present in optical wireless communications, a custom design imaging receiver is employed. In this work, we used the imaging receiver design proposed in [14] with 200 pixels. A detailed explanation about the calculation of the reception zone associated with each pixel is presented in [14]. The received optical signal obtained by each individual pixel can be separately amplified. A number of parameters such as the delay spread and SNR were inferred from the simulated impulse response.

1) The delay spread of an impulse response is given by [27], [28]:

$$D = \sqrt{\frac{\sum_{\forall i}(t_i-\mu)^2\ P_{ri}^2}{\sum_{\forall i} P_{ri}^2}} \tag{2}$$

where t_i is the time delay associated with the received optical power P_{ri}, and μ is the mean delay given by:

$$\mu = \frac{\sum_{\forall i} P_{ri}^2 t_i}{\sum_{\forall i} P_{ri}^2} \tag{3}$$

2) The SNR of the received signal can be written as [29]:

$$SNR = \left(\frac{R(P_{S1}-P_{S0})}{\sigma_0+\sigma_1}\right)^2, \tag{4}$$

R is the responsivity of the photodetector which in our case is chosen to be R = 0.6 A/W. This is a typical value for a silicon photodetector. P_{S1} and P_{S0} are the power levels associated with logic 1 and 0 respectively. The noises σ_1 and σ_0 associated with logic 1 and 0 respectively are given by:

$$\sigma_0 = \sqrt{\sigma_{pr}^2 + \sigma_{bn}^2 + \sigma_{s0}^2}\ \ and\ \ \sigma_1 = \sqrt{\sigma_{pr}^2 + \sigma_{bn}^2 + \sigma_{s1}^2} \tag{5}$$

σ_{pr}^2 represents the preamplifier noise which is a function of the design used for the preamplifier and σ_{bn}^2 represents the background shot noise component which is evaluated by computing the corresponding shot noise current. The noise component that is a direct result of the received signal power is composed of two elements. The shot noise component σ_{s0}^2 which is the noise associated with P_{s0} , is the first element, and σ_{s1}^2, associated with P_{s1}. is the second element. According to the experimental results reported in [30], this signal-dependent noise is very small and is often neglected. Calculations of the background shot noise can be found in [14], and higher bit rates of 1.25 Gb/s and 2.5 Gb/s are evaluated in our proposed systems. We used the preamplifier design proposed in [31].

4. Simulation Results

This section explores the performance of our proposed systems (HCD-IR and FABS-IR) under the impact of multipath dispersion, transmitter mobility and receiver noise. Comparison of the channel delay spreads of our proposed systems using different reception techniques, imaging and non-imaging receivers, is given in Fig. 4. The transmitter moves along the x=1 m line. The delay spread result of our imaging system is quoted when the system employs selection combining (SC) to select the imaging receiver pixel with the best SNR [14]. The non-imaging HCD-IR system shows much more signal delay

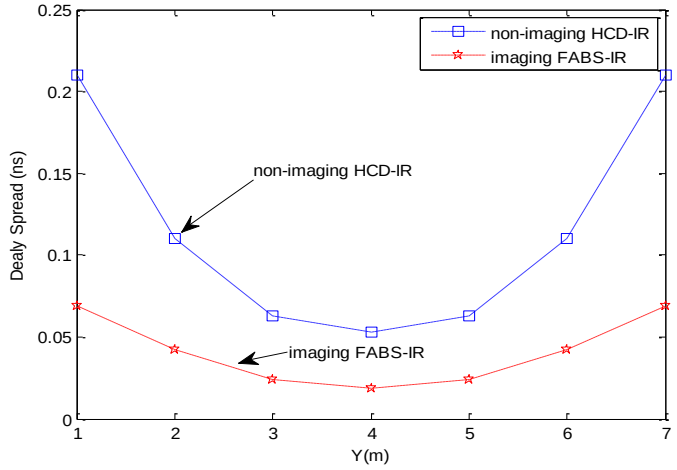

Fig. 4: The channel delay spread of our proposed systems employing non-imaging and imaging receiver, when the transmitter moves along the x=1m line.

spread due to the wide receiver FOV (FOV=90°) which accepts a wide range of rays with different path lengths from the transmitter to the receiver. The proposed beam steering IR system coupled with an imaging receiver decreases the delay spread from 0.22 ns to almost 0.07 ns. This is attributed to two reasons: firstly, due to the narrow FOV of each pixel, which limits the rays received by using 200 small FOV (about 11.3°). Secondly, due to the use of the adaptive beam steering technique.

The SNR evaluations of our proposed configurations: non-imaging HCD-IR and imaging FABS-IR systems are performed under the effect of transmitter mobility, receiver noise, and multipath propagation. The proposed system is set to operate at 1.25 Gb/s and 2.5 Gb/s with photodetector areas of 1 cm^2 (non-imaging receiver) and 1mm^2 (imaging and non-imaging receivers). A small detector area is needed to reduce the detector high capacitance, hence improving the receiver bandwidth. The SNR results of our imaging receiver are given when the system employs selection combining technique and are shown in Figs. 5 (a) and (b), when the transmitter moves near to the wall, at 1m steps along the x = 1 m line. The proposed HCD-IR with wide FOV receiver with 1 cm^2 detector area achieves around 4.4 dB SNR when the system operates at 1.25 Gb/s. However, the detector capacitance is proportional to its active area. This means that if the active area of the detector is large, such as 1 cm^2, the detector capacitance will be large, which results in a restriction in the achievable bandwidth. Therefore the detector active area has to be reduced at higher data rates. Reducing the detector area to 1mm^2 will lead to a reduction in SNR to about 40 dB. Also the 3-dB channel bandwidth of a wide FOV HCD-IR (at the room corner) is 0.79 GHz associated with 0.22 ns delay spread. This is clear evidence that our proposed system HCD-IR with wide

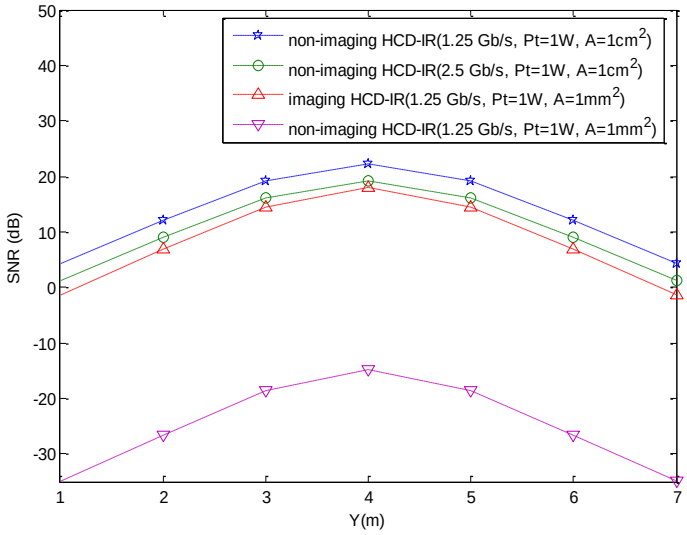

(a) HCD-IR

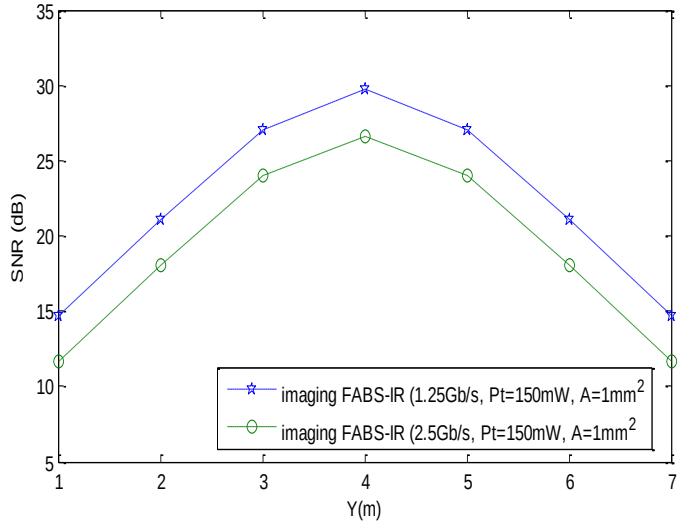

(b) FABS-IR

Fig. 5: The SNR results of our proposed system (a) non-imaging and imaging HCD-IR with total transmit power Pt= 1 W and (b) imaging FABS-IR with Pt=150 mW, when transmitter operates at 1.25 Gb/s and 2.5 Gb/s and moves along x=1m while the receiver is fixed at the centre of the ceiling.

non-imaging FOV receiver cannot operate at 1.25 Gb/s and 2.5 Gb/s. An imaging receiver can be used with HCD-IR system to resolve this problem. However, the link budget is still small due to the diffuse transmission (single wide beam). The SNR achieved in our imaging HCD-IR system is -1.4 dB, see Fig 5 (a). In order to overcome this issue, our new imaging diversity receiver coupled with fast beam steering

system FABS-IR is used. The FABS-IR configuration performs better than the HCD-IR. The proposed imaging FABS-IR system achieves around 14.7 dB and 11.7 dB SNR at 1.25 Gb/s and 2.5 Gb/s, respectively, under the effect of multipath dispersion, receiver noise and mobility, see Fig 5 (b). This is due to the use of (finite) adaptive beam steering as well as imaging diversity receiver. Adaptive beam steering has the ability to move the beam near to the receiver in the presence of user mobility. Forward error correction (FEC) can also be used to reduce the BER form 10^{-6} to 10^{-9} in our FABS-IR proposed imaging system.

Through the use of our beam steering and computer generated holograms in IR uplink design, substantial SNR enhancement was achieved. The efficiency of the proposed FABS-IR is evaluated by examining time complexity. To examin the computational complexity of algorithms, the nature of a function T(m) [30] can be utilised. For instance, a linear algorithm of input size m can generate a linear time complexity of T(m) = {O} (m). An acceptable performance is obtained in a single pass implementation algorithm with complexity order of O(m), when there is a small value of m. however, a large value of m causes it to become too complicated. By scanning all the areas above, the classical beam steering with computer generated holograms [19] can identify the optimum hologram. It has the features of "one-pass" algorithms. Our classical computer generated holograms, therefore, have a linear time complexity and can be given as T(m) = {O}(m), in which m representing the total number of regions that should be covered for each transmitter. By increasing the value of m, significant SNR improvements are realized, but time complexity greatly increases due to the total number of holograms required, m. However, the FABS-IR is a recursive algorithm based on the D&C method, where the process to find the optimum hologram is recursively broken down into a number of iterations S. For example, in the case of four iterations (S=4), time complexity can be given as [32]:

$$T(m) = ST\left(\frac{m}{64}\right) + Sj = ST\left(\frac{m}{j2^{S}}\right) + Sj$$

$$log\left(\frac{m}{j}\right) T(1) + j\, log\left(\frac{m}{j}\right) = j\, log_2\left(\frac{m}{j}\right) \quad (6)$$

where *j* is the number of sub-problems (quadrants in our FABS-IR). The transmitter divides the stored holograms into four quadrants (i.e., j = 4) in each iteration. For example, in the case of m =512 (number of regions), the number of holograms needed for classical computer generated holograms beam steering is 512. In addition, the computation time required to identify the optimum holograms is 512 ms (if each SNR computation is carried out in 1 ms, based on typical processor). Alternatively, in the fast adaptive algorithm, the computation time needed to identify the optimum holograms is only 28 ms (solely four iterations are required). It should be noted that computation time in the fast algorithm is totally depends on number of holograms and the way that we divide them (in our case j=4). However, under different scenarios the computation time may be slightly changed.

5. Conclusions

In this paper, we proposed a new design of indoor uplink VLC systems using IR links. The advantage of such a system is the ability to add capacity with VLC channels acting as downlinks only while employing a full uplink capability in the form of an IR channel. We proposed a new method that uses fast adaptive beam steering (FABS-IR) coupled with imaging receivers to improve the system performance at high transmission rates (1.25 Gb/s and 2.5 Gb/s). The proposed FABS-IR can effectively steer the uplink channel in VLC systems closer to the receiver position. The FABS-IR are pre-calculated and stored in our proposed system without adding any complexity at the transmitter to reproduce (compute) the holograms. Increasing the number of holograms/regions helps the transmitter accurately identify the receiver's location, hence improving the system performance. In order to select the best pre-calculated hologram in a shorter amount of time, a search algorithm based on D&C was used. In the worst communication path considered, when the ceiling is divided into 512 regions (512 holograms are pre-calculated and stored in

the system), at each transmitter and receiver location our proposed system, FABS-IR, reduces the time needed to identify the optimum hologram position from 512 ms for the classical configuration to about 40 ms. The proposed FABS-IR system coupled with an imaging receiver obtained around 14.7 dB and 11.7 dB SNR at 1.25 Gb/s and 2.5 Gb/s as exhibited in the simulation results. In addition, the proposed system significantly decreases the channel delay from 0.22 ns in wide HCD-IR to about 0.07 ns.

6. References

1- Komine, T., Haruyama, S. and Nakagawa, M., 'Performance evaluation of narrowband OFDM on integrated system of power line communication and visible light wireless communication', 1st International Symposium on Wireless Pervasive Computing, 2006, pp.1- 6.

2- Komine, T., Nakagawa, M. 'Fundamental analysis for visible-light communication system using LED lights', IEEE Trans. Consum. Electron., 2004, 50, (1), pp 100–107.

3- Le Minh, H., O'Brien, D., Faulkner, G., Zeng, L., Lee, K., Jung, D., & Oh, Y. 'High-speed visible light communications using multiple-resonant equalization', IEEE Photonics Technology Letters, 2008, 20, (14), pp 1243-1245.

4- Wang, C. X., Haider, F., Gao, X., You, X. H., Yang, Y., Yuan, D. & Hepsaydir, E. 'Cellular architecture and key technologies for 5G wireless communication networks', IEEE Communications Magazine, 2014, 52, (2), pp 122-130.

5- Green, R. J., Joshi, H., Higgins, M. D., & Leeson, M. S. 'Recent developments in indoor optical wireless communications', IET communications, 2008, 2, (1), pp 3-10.

6- Hussein, A. T., & Elmirghani, J. M. H. 'A survey of optical and terahertz (THz) wireless communication systems', IEEE Commun. Surv. & Tutorials, 2016, pp 1-27.

7- Tsonev, D., Chun, H., Rajbhandari, S., McKendry, J. J., Videv, S., Gu, E. & Dawson, M. D. 'A 3-Gb/s Single-LED OFDM-Based Wireless VLC Link Using a Gallium Nitride', IEEE Photonics Technology Letters, 2014, 26, (7), pp 637-640.

8- Hussein, A. T., & Elmirghani, J. M. 'Mobile multi-gigabit visible light communication system in realistic indoor environment', Journal of Lightwave Technology, 2015, 33, (15), pp 3293-3307.

9- Hussein, A. T., & Elmirghani, J. M. 'High-speed indoor visible light communication system employing laser diodes and angle diversity receivers', In 17th International Conference on Transparent Optical Networks (ICTON), 2015, pp. 1-6.

10- Hussein, A. T., & Elmirghani, J. M. 'Performance evaluation of multi-gigabit indoor visible light communication system', 20th European Conference on Networks and Optical Communications (NOC), 2015, pp. 1-6.

11- Hussein, A. T., & Elmirghani, J. M. '10 Gbps Mobile Visible Light Communication System Employing Angle Diversity, Imaging Receivers, and Relay Nodes', Journal of Optical Communications and Networking, 2015, 7, (8), pp 718-735.

12- Shao, S., Khreishah, A., Rahaim, M. B., Elgala, H., Ayyash, M., Little, T. D., & Wu, J. 'An indoor hybrid WiFi-VLC internet access system', 11th International Conference on Mobile Ad Hoc and Sensor Systems, 2014, pp. 569-574.

13- Yuanquan, W., & Nan, C. ‘A high-speed bi-directional visible light communication system based on RGB-LED’, China Communications, 2014, 11, (3), 40-44.
14- Alresheedi, M. T., & Elmirghani, J. M. ‘10 Gb/s indoor optical wireless systems employing beam delay, power, and angle adaptation methods with imaging detection’, Journal of Lightwave Technology, 2012, 30, (12), pp 1843-1856.
15- Alresheedi, M. T., & Elmirghani, J. M. ‘Performance evaluation of 5 Gbit/s and 10 Gbit/s mobile optical wireless systems employing beam angle and power adaptation with diversity receivers’, IEEE Journal on Selected Areas in Communications, 2011, 29, (6), pp 1328-1340.
16- Alresheedi, M. T., & Elmirghani, J. M. ‘Hologram selection in realistic indoor optical wireless systems with angle diversity receivers’, Journal of Optical Communications and Networking, 2015, 7, (8), pp 797-813.
17- Alsaadi, F. E., & Elmirghani, J. M. ‘High-speed spot diffusing mobile optical wireless system employing beam angle and power adaptation and imaging receivers’, Journal of Lightwave Technology, 2010, 28, (16), pp 2191-2206.
18- Hussein, A. T., Alresheedi, M. T., & Elmirghani, J. M. ‘20 Gb/s Mobile Indoor Visible Light Communication System Employing Beam Steering and Computer Generated Holograms’, Journal of Lightwave Technology, 2015, 33, (24), pp 5242-5260.
19- Hussein, A. T., Alresheedi, M. T., & Elmirghani, J. M. ‘Fast and Efficient Adaptation Techniques for Visible Light Communication Systems ’, Journal of Optical Communications and Networking, 2016, 8, (6), pp 382-397.
20- Gfeller, F. R., & Bapst, U. ‘Wireless in-house data communication via diffuse infrared radiation’, Proceedings of the IEEE, 1979, 67, (11), pp 1474-1486.
21- Haigh, P. A., Son, T. T., Bentley, E., Ghassemlooy, Z., Le Minh, H., & Chao, L. ‘Development of a visible light communications system for optical wireless local area networks’, In Computing, Communications and Applications Conference (ComComAp), 2012, pp. 351-355.
22- Wong, K. K., & O'Farrell, T. ‘Spread spectrum techniques for indoor wireless IR communications’, IEEE Wireless Communications, 2003, 10, (2), pp 54-63.
23- Pohl, V., Jungnickel, V., & Von Helmolt, C. ‘Integrating-sphere diffuser for wireless infrared communication’, IEE Proceedings-Optoelectronics, 2000, 147, (4), pp 281-285.
24- Le Minh, H., O'Brien, D., Faulkner, G., Bouchet, O., Wolf, M., Grobe, L., & Li, J. ‘A 1.25-Gb/s indoor cellular optical wireless communications demonstrator’, IEEE Photonics Technology Letters, 2010, 22, (21), pp 1598-1600.
25- Wang, K., Nirmalathas, A., Lim, C., & Skafidas, E. ‘High-speed optical wireless communication system for indoor applications’, IEEE Photonics Technology Letters, 2011, 23, (8), pp 519-521.
26- Fadlullah, J., & Kavehrad, M. ‘Indoor high-bandwidth optical wireless links for sensor networks’, Journal of lightwave technology, 2010, 28, (21), pp 3086-3094.
27- Al-Ghamdi, A., & Elmirghani, J. M. ‘Optimization of a triangular PFDR antenna in a fully diffuse OW system influenced by background noise and multipath propagation’, IEEE transactions on communications, 2003, 51, (12), pp 2103-2114.
28- Al-Ghamdi, A. G., & Elmirghani, J. M. ‘Line strip spot-diffusing transmitter configuration for optical wireless systems influenced by background noise and multipath dispersion’, IEEE Transactions on Communications, 2004, 52, (1), pp 37-45.
29- Desurvire, E., & Zervas, M. N. ‘Erbium-doped fiber amplifiers: principles and applications’, Physics Today, 1995.
30- Moreira, A. J., Valadas, R. T., & de Oliveira Duarte, A. M. ‘Optical interference produced by artificial light’, Wireless Networks, 1997, 3, (2), pp 131-140.
31- Leskovar, B. ‘Optical receivers for wide band data transmission systems’, IEEE Transactions on Nuclear Science, 1989, 36, (1), pp 787-793.
32- Kleinberg, J., & Tardos, E. ‘Algorithm design’, Pearson Education India, 2006.